



	<b><sup>2</sup>Experiment title:</b> <b>Finite size effect on the <math>\alpha/\beta</math> phase transition in MnAs patterned thin films</b>	<b>Experiment number:</b> HE-2965
<b>Beamline:</b> ID-01	<b>Date of experiment:</b> from: 8/07/2009 to: 14/07/2009	<b>Date of report:</b> 14-07-2009
<b>Shifts:</b> 19	<b>Local contact(s):</b> Dr. Dina CARBONE	<i>Received at ESRF:</i>

**Names and affiliations of applicants** (\* indicates experimentalists):

Dr. Cristian MOCUTA, Synchrotron SOLEIL, France (\*)  
Dr. Antoine BARBIER, CEA-Saclay, France (\*)  
Mr. Souliman EL MOUSSAOUI, Synchrotron-SOLEIL, France (\*)  
Dr. Stefan STANESCU, Synchrotron SOLEIL, France (\*)  
Dr. Rachid BELKHOU, Synchrotron-SOLEIL, France (\*)  
Dr. Fumiyoshi TAKANO, AIST, Tsukuba, Japan  
Dr. Hiro AKINAGA, AIST, Tsukuba, Japan  
Prof. Ernst BAUER, Arizona State University, Dpt. of Physics, Arizona, USA  
Dr. François MONTAIGNE, Université Nancy I, France

**Report: (preliminary)**

Ferromagnetic MnAs is a promising candidate for electrical spin injection into GaAs and Si based semiconductors. It exhibits a large carrier spin polarization, small coercive field and relatively high saturation magnetization and Curie temperature. Bulk MnAs is ferromagnetic (FM) at room temperature (RT) ( $\alpha$  phase) and shows close to 40°C a first order transition to the paramagnetic  $\beta$  phase. On the contrary, epitaxial MnAs films on GaAs substrate, which are more appropriate for the injection applications, show at (RT) the coexistence of both phases. This effect has been widely studied by our group in the last years by X-PEEM and LEEM microscopy. The phase coexistence results in the formation of self-organized stripes of alternating  $\alpha$  and  $\beta$  phases. The phase coexistence is due to anisotropic strain applied by the GaAs substrate.

Going one step further and in the course of miniaturizing a unit cell for magnetic device, one may wonder how the system magnetically reorganizes when the associated energies become smaller than the thermal energy  $k_B T$ . In the particular case of MnAs patterns, the question arises what is the effect of the finite size on the strain release induced by the substrate and on the  $\alpha/\beta$  coexistence regime thin films? Recent micro-diffraction measurements made by our group on a similar system (Magnetic Tunnel Junctions) (see experimental reports HS-2971, HS-3636 and [1]) have shown that patterned samples can have very different micromagnetic behavior and therefore we cannot simply extrapolate the results of thin films to patterned objects.

In the present experiment, the sample consisted of rectangles and disks of epitaxial MnAs grown on GaAs(001) patterned by electron lithography. The 300nm thick films were grown by MBE at the AIST laboratory (Japan) and the electron-beam lithography process was performed at the Nancy facility. In this experiment we have investigated the temperature dependence of the  $\alpha/\beta$  transition with respect to the patterned object size and shape. On a lithographed sample with several motifs (**fig. 1**), we have investigated in this experiment squares and rectangles of sizes of  $12\text{ }\mu\text{m} \times 12\text{ }\mu\text{m}$ ,  $3\text{ }\mu\text{m} \times 3\text{ }\mu\text{m}$ ,  $2.25\text{ }\mu\text{m} \times 2.25\text{ }\mu\text{m}$ ,  $1.5\text{ }\mu\text{m} \times 1.5\text{ }\mu\text{m}$ ,  $0.75\text{ }\mu\text{m} \times 0.75\text{ }\mu\text{m}$ ,  $0.75\text{ }\mu\text{m} \times 2.25\text{ }\mu\text{m}$ ,  $2.25\text{ }\mu\text{m} \times 0.75\text{ }\mu\text{m}$  as shown in **fig. 1**.

Beamline setup : 23 Be compound refractive lenses (CRL) were used to focus down the beam, of primary energy  $E=8.25\text{ keV}$ , to a size of  $1.5\text{ }\mu\text{m} \times 3\text{ }\mu\text{m}$  (HxV) full width half maximum (FWHM) and a measured

photon flux in the spot of  $1.5 \times 10^{10}$  ph/s. The Be lenses were installed on an alignment stage before the sample which was mounted on a Peltier cooling/heating device developed by the ID01 beamline staff and the sample environment pool. This device allowed accessing easily a  $-18^\circ\text{C}$  to  $+74^\circ\text{C}$  temperature range. The temperature stability turned out to be excellent with a regulation overshoot limited to 5 mK when using a  $5^\circ\text{C}/\text{min}$  temperature ramp. During the experiment the sample was kept under He flow to prevent oxidation and intensity loss due to the absorption by air. The sample was mounted horizontally with diffraction happening in the vertical plane. An avalanche photon diode (APD) detector was used at a distance of 900 mm from the sample and the reciprocal space resolution ( $8.2 \times 10^{-3} \text{ \AA}^{-1}$  in  $q_{\text{perp}}$  direction) was obtained through a set of  $1 \text{ mm} \times 4 \text{ mm}$  slits ( $v \times h$ ) placed in front of the detector ( $0.064^\circ$  opening in vertical direction).

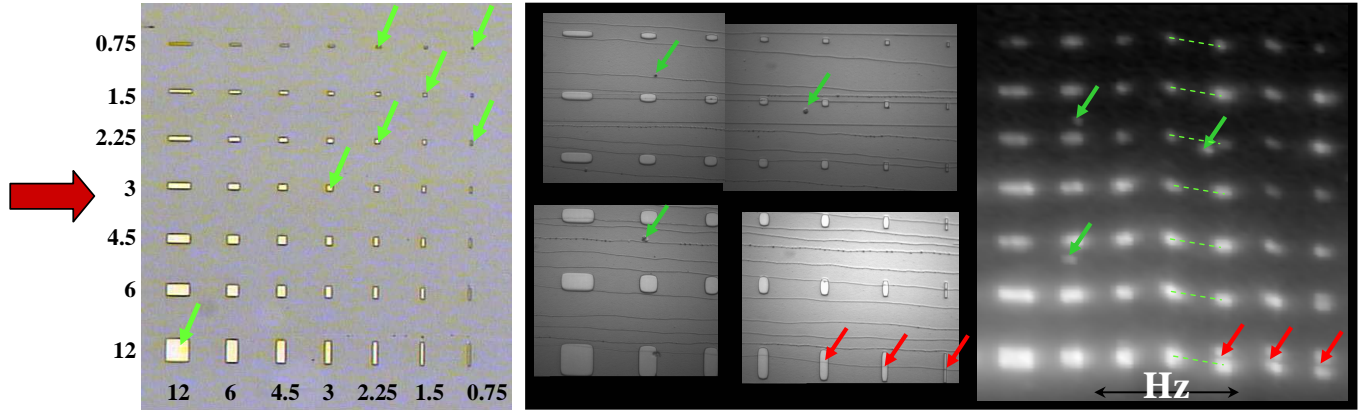


**Figure 1:** (left) Optical image of the lithographed sample. The corresponding dots sizes (for each row and respectively column) are shown, in  $\mu\text{m}$ . The measured dots are highlighted by arrows. X-ray beam is coming from the left side (red arrow), and the  $\alpha/\beta$  stripes are perpendicular to the beam vertical direction in the figure); (right) 2d cartography performed for the sample with the diffractometer angles set such that the sample is in Bragg condition (alpha phase). Some lithography defects are also present and marked (by colored arrows) on the 2d map and on the insets of the optical image. Note the presence of wobble of one of the motor stages (hz, cf. dotted lines) used for displacement of the sample; this required the use of time consuming automatic alignment procedures when changing the investigated dot (see text); with the risk of finding the neighbor dot.

After cycling the sample in a temperature range from 0 to  $60^\circ\text{C}$ , (2 times in order to release the growth strain), a 2d cartography (using a characteristic diffraction signal, see exp. report HS-3632 and [2]) of the sample was performed. Compared with an optical image of the sample (**fig.1**), it allowed identifying the region of interest and extracting the positions used later on for an automatic alignment of each structure. Then the hysteresis in temperature was measured for each considered square/rectangle (dot): 2 wide alignment scans at the Bragg positions (in specular diffraction geometry) of the  $\alpha/\beta$  phases were performed to center the dot with respect to the incident beam (these scans could be largely reduced or removed for a better suited microdiffraction goniometer head). Then specular and rocking scans were performed for the  $\alpha$  and  $\beta$  Bragg peaks. From these measurements the temperature hysteresis and the strain relaxation can easily be extracted (**fig. 2**). About 20 temperatures in the  $8 - 60^\circ\text{C}$  range were considered (heating and cooling down). We should note here that the global output of the experiment could be optimized (increased) by increasing the speed of the goniometer motors as well. The typical counting time for the smallest (largest) Bragg reflection was 0.6 sec (0.3 sec respectively) for a total acquisition time per point of more than 2 sec.

We observe large variations in temperature for the onset of transition depending on the shape and size of the dots. The widths of the hysteresis loops also largely depend on the dot sizes/shapes. These effects are related to the finite phase stripe widths and their orientation ( $//$  or perpendicular) with respect to the shape for the rectangles. More work is needed to link these results with the elastic constants of the materials. Further experiments will be needed to establish a statistical investigation of the temperature behaviors of the dots with respect to their initial state (amount of  $\alpha/\beta$  phases).

In summary, the experiment was very successful and the ID01 setup proved to be well suited to tackle this topic.

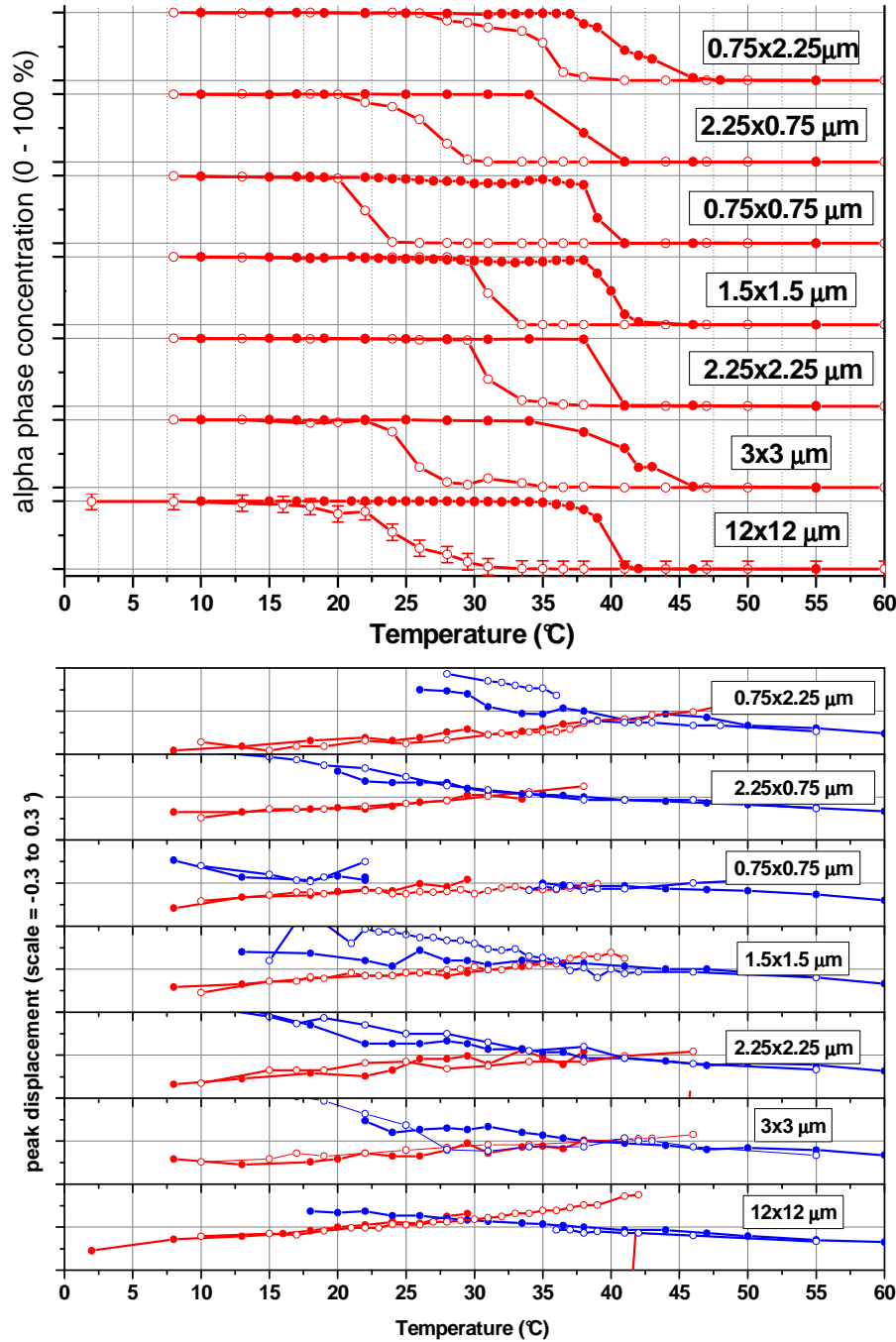


**Figure 2 (preliminary):** (top) Estimation of the concentration of the  $\alpha$ -phase, deduced from the ratio of peak intensity characteristic for the  $\alpha$  and  $\beta$  phases respectively (the corrected and integrated intensity considering also the rocking scans were measured and will be extracted during a thorough exploiting of the data). The horizontal grey lines define the 0-100 % range for each dot. Error bars are shown only for the 1<sup>st</sup> curve. The 1<sup>st</sup> dimension reported for each dot is the one along the beam direction. The heating (filled symbols) and cooling down (opened symbols) curves are shown. (bottom) Shift of the peak position corresponding to the  $\alpha$  (red) and  $\beta$  (blue) phases respectively, for heating (open symbols) and cooling down (filled symbols). A later data analysis will consider as well the presence of split peaks for temperatures close to the phase transition.

[1] C. Mocuta *et al.*, Appl. Phys. Lett. **91** 241917 (2007); Eur. Phys. J. Special Topics **167**, 53–58 (2009).  
 [2] C. Mocuta *et al.*, Phys. Rev. B. **77** (2008) 245425.